Physical and Mechanical Properties of Nanocomposite Barrier Film Containing Encapsulated Nanoclay

Mojgan Mirzataheri, Mohammad Atai, Ali Reza Mahdavian

Polymer Science Department, Iran Polymer and Petrochemical Institute, Tehran, Iran

Received 21 July 2009; accepted 17 April 2010
DOI 10.1002/app.32711
Published online 13 July 2010 in Wiley InterScience (www.interscience.wiley.com).

ABSTRACT: Waterborne poly(styrene-*co*-butyl acrylate) was prepared via miniemulsion polymerization in which nanoclay (Cloisite® 30B, modified natural MMT) in different concentrations was encapsulated. Scanning electron microscopy, X-ray diffraction, and transmission electron microscopy confirmed the encapsulation and intercalated-exfoliated structure of Cloisite® 30B within poly(styrene-*co*-butyl acrylate). The effect of nanoclay content on water vapor permeability, water uptake, oxygen permeability, thermal, and mechanical properties of thin films containing 1.5, 2.56, 3.5, and 5.3 wt % encapsulated Cloisite® 30B in poly(styrene-*co*-butyl acrylate) was investigated. The presence of encapsulated Cloisite® 30B within the polymer matrix improved tensile strength, Young's modulus, and toughness of the nanocomposites depending on the nanoclay content. Water vapor transmission rate, oxygen barrier properties, and thermal stability were also improved. The results indicated that the incorporation of Cloisite® 30B in the form of encapsulated platelets improved physicomechanical properties of the nanoclay-polymer composite barrier films. © 2010 Wiley Periodicals, Inc. J Appl Polym Sci 118: 3284–3291, 2010

Key words: miniemulsion; nanocomposite; Cloisite® 30B; barrier properties; physicomechanical properties

INTRODUCTION

Studies proved that hybrids of polymer-clay structure, with exfoliated platelets of dispersed nanoclay within a polymer matrix showed outstanding physicomechanical and barrier performances because of the high aspect ratio of the nanoclay and further increase in tortousity of the diffusion path against the penetrant.[1–3] The enhanced performances including reduced gas permeability, better thermal stability, and flame retardancy, higher modulus and conductivity, are the results of the larger surface-to-volume ratio of nanoclay particles. Because of the high surface area and high stress transfer efficiency, these hybrid materials provide improvements in the properties of polymer matrices with high clarity and lower price at very low loading fractions (1–5%) in comparison with the higher loadings (30–50%) of macrosize fillers, which normally are used in the conventional composites.[4–7] Of the nanoparticles, which have been used in the nanocomposites are clay, carbon nanotubes, graphites, silica, gold, alumina, antimony/tin oxide, silver/zinc oxide, copper oxide, and indium/tin oxide.[8]

In recent years, polymer-layered silicate nanocomposites have significantly been attracted in academic research and industrial applications[9] especially in coating industries. The improvement in the performance of the coatings depends on the surface area, aspect ratio, extent of dispersion and orientation and finally on the interfacial interaction of the layered silicates within the polymer matrix.[10–12] Montmorillonite (MMT) is a platy structure material with broad aspect ratio and size distribution. As it is a hydrophilic clay and thermodynamically incompatible with most hydrophobic polymers of commercial importance,[13] organic modification of the intergalleries alkali cations of the clay by replacement with organic cations is required[14] to let the polymer molecules penetrate into the clay basal interspacing.

Barrier property is one of the most important properties for paper coating purposes.[1,15,16] Attempts have been made to improve barrier efficiency of polymers by using water-based latex containing MMT nanoplatelet dispersion. The platelet structure of the nanoparticles increases the tortuosity of the path for the diffusion of oxygen, water, and other gases and liquids[17] throughout the nanocomposite. These layered silicate/polymer nanocomposites, as advanced materials, have also been reported to offer high stiffness and high heat resistant superior to conventional reinforced composites attributed to the high surface area between the silicate layers and polymeric material.[10,18]

One of the potential applications of the nanoclay composites in the form of waterborne latexes lies in the paper industries as coating binders. The film-forming ability, the physical and mechanical properties and barrier performance of the binders are of

Correspondence to: M. Atai (m.atai@ippi.ac.ir).

© 2010 Wiley Periodicals, Inc.

great importance for the coating applications.[19,20] As in thermoplastic matrixes, increase in modulus through incorporation of fillers generally results in toughness drop, researchers are interested in improving the toughness-to-stiffness balance in polymeric nanomaterial.[21,22]

Styrene-acrylate, styrene-butyl acrylate, and styrene-butadiene latexes are widely used as binders in paper coatings,[23] due to good adhesion (for most substrates), flexibility, outdoor durability (resistance to UV degradation and yellowing), and reasonable cost. But waterborne nanocomposite latexes containing encapsulated nanoclay within the polymer matrix[24] have not been studied in coating applications. In this study, physical and mechanical properties of nanoclay-encapsulated composites, prepared via miniemulsion polymerization of poly(styrene-*co*-butyl acrylate) in the presence of Cloisite® 30B, were investigated. The butyl acrylate in copolymer may improve adhesion properties due to its low glass transition temperature, whereas styrene can increase mechanical properties of the polymer film. The effect of nanoclay content on the nanocomposite properties, such as barrier performances, thermal stability, thermomechanical behavior, tensile strength, stiffness, and toughness were also studied.

MATERIALS AND METHODS

Materials

Reagents were analytical grade and were used as received. Cloisite® 30B commercially available organoclay, (with $d_{001} = 1.74$ nm measured in our work), a natural MMT modified with an organic modifier named: methyl tallow bis-2-hydroxyethyl quaternary ammonium chloride (MT2EtOHCl) was supplied by Southern Clay Products (Gonzales, USA) that was further ground by mortar and pestle. Na_2CO_3 (Arastoo, Iran) used as buffer. Sodium dodecyl sulfate (SDS) from Aldrich, hexadecane (99%), styrene (99%), and Span 80 from Merck Chemical and butyl acrylate (99%) from Fluka Chemical were purchased and used as received. 2,2′-Azobisisobutyronitrile (AIBN, Fluka) was used as initiator. Styrene was purified by two times washing with 5% aqueous NaOH solution (W/V) and rinsing with plenty of distilled water until pH of the separated aqueous phase was reached 7.0 and kept on dried $CaCl_2$ at 0°C before use.

Methods

Preparation of nanocomposite latexes

Latex particles containing encapsulated Cloisite® 30B were synthesized by the procedure reported elsewhere.[24] Briefly, styrene (12.73 g), Cloisite® 30B (1 g), Span 80 (0.10 g), butyl acrylate (6.27 g), and hexadecane (1.14 g) was magnetic stirred under 300 rpm for 1 h at room temperature and then sonicated for 2 min. Meanwhile, aqueous phase containing distilled water (78 g) and Span 80 (0.20 g) was prepared. The monomer and aqueous phases were mixed under vigorous magnetic stirring for 15 min. Then SDS (0.2 g) was added to the above dispersion and further homogenization and ultrasonication was conducted with the sonicator probe for 4 min. The obtained miniemulsion with solids content of 20% was used for subsequent polymerization. AIBN (0.28 g) was added to the as-prepared miniemulsion in a four-necked 250 mm glass reactor equipped with condenser, and subsequently degassed by N_2 at room temperature for 30 min. The polymerization of the miniemultion was conducted in a water bath at 60°C. The reaction was then terminated by adding one drop of 1% (*W/V*) hydroquinone solution in methanol. Concentrated milky latex with final conversion of 95.4% and 1 wt % coagulum content was obtained.[24]

Preparation of hot pressed free film

The prepared latexes were coagulated and dried under vacuum. Free films of the nanoclay containing composites were prepared by using a hot press (D. ALEEY, Iran) at 240–250°C and 100–120 bar pressure. The films were dried at 40°C under vacuum for 24 h. Test specimens were then cut out from these films.

Characterization

X-ray diffraction (XRD) patterns were recorded on a Siemens D5000 (Germany) using Cu kα ray ($\lambda = 1.54056$ Å) as the radiation source, with a step size of 0.02° and a scan step time of 1 s. The d_{001} basal spacing of the samples were calculated using the Bragg equation ($d = \lambda/2 \sin \Theta$, where Θ is the diffraction angle and λ is the incident wavelength (1.54056 Å)). Transmission electron microscopy (TEM) observations on the morphology of latex particles were conducted on a CEM-902A, Zeiss (Germany) at an accelerating voltage of 80 kV. The samples were prepared by casting a drop of 40 times diluted latex solution onto a 200-mesh covered Formvar/carbon-coated copper grid at room temperature and dried at 60°C overnight.

Oxygen Transmission Rate (OTR) was tested using Brugger (GDP-C) O_2-permeability tester (Munchen, Germany) according to ASTM D1434-82 (Determining gas permeability characteristics of plastic film), method A. In this instrument (GDP-C software calculates with one bar pressure difference) the sample is located between the top and bottom sections of

the permeation cell and the volume of the bottom part is as small as possible. Before each test the bottom part of the permeation cell is evacuated and during testing the top part is filled with the test gas. The gas permeating the material causes a pressure increase at the bottom part of the permeation cell which is evaluated and displayed by an external computer. The test method A (Gas constant-Evacuation Top/Bottom) can obtain exact results quickly as this method evacuates the space above and below the sample. Then the permeation at the bottom surface is measured by the evaluation of the pressure increase within the measuring unit. The values are read by a high resolution A-D converter to display gas transmission rates.

The water vapor barrier permeability test was measured by the gravimetric cup method according to the ASTM E-96 in a temperature controlled chamber at 30°C, which was kindly provided by the Faculty of the Chemical Science, University of the Basque Country, San Sebastian (Spain). The latex free film was placed in the upper part of a cell containing a certain amount of water and then it was well-sealed so that water could only permeate through the free film. The water vapor transmission rate (WVTR, g mm/cm^2 days) was calculated as follows:

$$\mathrm{WVTR} = 8.64 \times 10^5 \times AB/[C(1-D)]$$

where A is the slope of the water vapor loss in time (g/s), B is the thickness of the free film (mm), C is the surface area of the free film ($C = 2.54$ cm^2), and D is water vapor activity.[10]

Water uptake of the as-prepared latex films was measured according to the following procedure: the dry films were weighed (m_1) and immersed in deionized water for 48 h. After the storage in water, the films were blot-dried and weighed (m_2).[18,23] The water uptake was then calculated as follows:

$$\text{Water uptake } (\%) = \frac{m_2 - m_1}{m_1} \times 100$$

which represents the adsorbed water percentage on the surface and absorbed into the nanocomposite.

Thermal stability was determined using TGA 1500 (Polymer Laboratories, UK) thermogravimetric analyzer. The samples were heated at a scan rate of 10°C/min from room temperature to 600°C in N_2 atmosphere. The reported values are the average of three repeats. The stress–strain behavior of the nanocomposites was observed by a universal testing machine (SMT 20, Santam, Iran) with a crosshead speed of 2 mm/min. Each specimen had the dimensions of 0.15 mm thickness, 12–13 mm width, and 50 mm length measured by digital micrometer (LAI03, Mitutoyo, Japan). The tests were carried out at 25 (±1)°C and 50% relative humidity. The reported values are the average of 10 measurements based on ASTM D-2370. The results were then statistically compared using one-way ANOVA and Tukey post hoc test at a significance level of 0.05.

Scanning electron microscopy (SEM) analysis was carried out on a TESCAN model VEGAII XMU (Czech Republic). The samples were gold coated in high vacuum mode (30 kV, 20 μA) with thickness less than 3 nm in less than 3 min and working vacuum pressure of 9.9×10^{-3} Pa inside the chamber to dry the sample before gold coating.

Dynamic mechanical thermal analyzer DMA-TRITON, Tritec 2000 DMA was used in tension mode to study the temperature dependence of storage modulus (E') and tanδ of nanocomposites containing 1.5, 2.56, 3.5, 5.3 wt % Cloisite® 30B. The specimens used were rectangular in shape and approximate dimensions of 10 × 5 × 0.1 mm (length, width, thickness). The dynamic temperature ramp test was done at a vibration frequency of 1 Hz, displacement of 0.025 mm, heating rate 5°C/min with the temperature range from −50°C to 200°C at a strain of 1%. Glass transition temperature of the specimens was obtained from the onset of modulus drop.

RESULT AND DISCUSSION

Structure of nanocomposites, X-ray, and TEM results

The final waterborne latex synthesized through miniemulsion polymerization was powdered off in the liquid nitrogen, dried, and used for XRD measurement. Cloisite® 30B has an interlayer spacing of 1.74 nm at 2Θ about 5.08° calculated from Bragg equation (d_{001} is the interplanar distance of (001) reflection plane). The XRD patterns of pristine Cloisite® 30B and its nanocomposites are shown in Figure 1 in which sharp peak of Cloisite® 30B (appears at 5.08°) shifted to lower 2Θ angles with substantial reduction in the intensities of the peak for the nanocomposites containing Cloisite® 30B. This implies exfoliation of Cloisite® 30B in the final nanocomposite.[24]

These nanocomposite particles were mainly composed of spherical particles in a range of 100–300 nm.[24] For verifying the morphology of the obtained nanocomposite particles and exfoliation of Cloisite® 30B, TEM micrographs were taken. One of the samples was dried at room temperature [Fig. 2(a)] and the other one was heated about 80°C to form a thin film on the grid [Fig. 2(b)]. These micrographs (polymer particles and polymer film respectively) were indicative of encapsulation and exfoliation of Cloisite® 30B platelets, dispersed well within the latex particles, which were prepared via miniemulsion polymerization with lack of clay armored

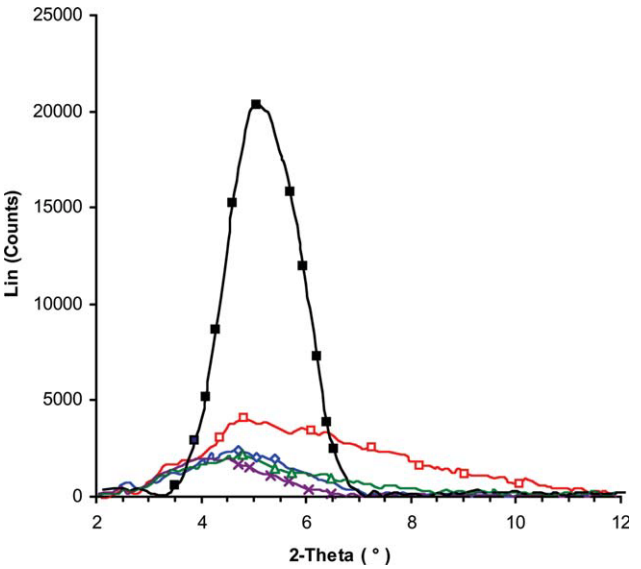

Figure 1 XRD patterns of Cloisite® 30B and poly(styrene-*co*-butyl acrylate)-Cloisite® 30B nanocomposites containing different nanoclay contents: Coisite 30B® (■), 1.5 wt % nanoclay (◊), 2.56 wt % nanoclay (×), 3.5 wt % nanoclay (□), 5.3 wt % nanoclay (▲).[24] [Color figure can be viewed in the online issue, which is available at www.interscience.wiley.com.]

latex particle.[24] Therefore X-ray and TEM analysis confirmed the presence of homogeneously dispersed Cloisite® 30B platelets in the copolymer matrix.

Oxygen permeability

Many foods and encapsulated medical products are sensitive to the climate and surrounding conditions, in particular to oxygen and water vapor and the quality of these products are adversely affected by the diffusion of the permeants. Therefore, packaging materials should have barrier functions against water vapor, oxygen and many other gases, and liquids.[25] The two most technical data used for barrier polymeric materials with major performance in the paper and packaging industries are oxygen and water vapor transmission rate.[26] For improving barrier properties usually plate-like fillers, such as clay, talc, or calcium carbonate, are added to the polymeric matrixes. Silicates having layered structure can effectively increase the vapor diffusion path length.[27,28]

The results (Table I) shows that the film prepared from the nanocomposite of Cloisite® 30B encapsulated in poly(styrene-*co*-butyl acrylate) exhibited improved oxygen barrier properties. Increasing Cloisite® 30B content, the barrier performance greatly increased and provided an oxygen transmission rate of about 240 (cm^3/m^2 24 h) for 5.3 wt % encapsulated Cloisite® 30B in comparison with the neat copolymer, which had an oxygen transmission rate of 1550 (cm^3/m^2 24 h). Hence, several time reductions were observed at 23°C and 50% relative humidity. As the permeants predominantly diffuse through amorphous areas of polymer, crystallinity is an important factor affecting the permeability (the higher the degree of crystallinity, the lower is the permeability of the polymer). During the thermal analysis no melt temperature or crystallization temperature was observed for our neat copolymer and

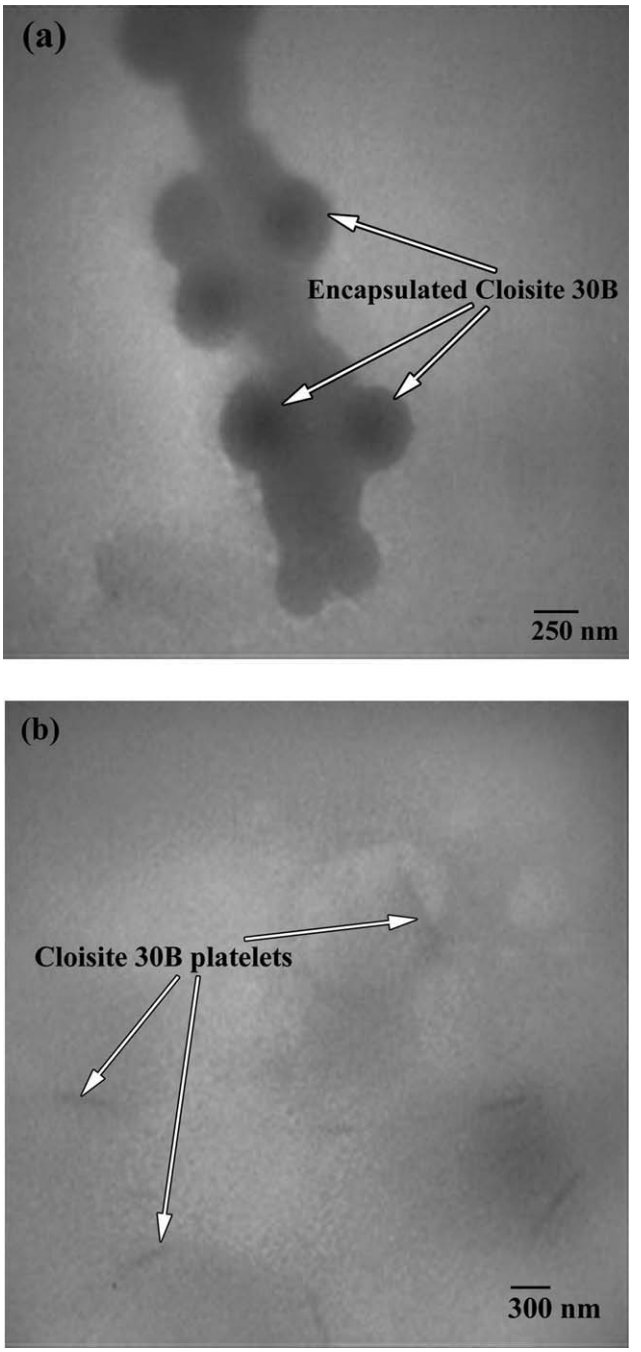

Figure 2 TEM micrographs of poly(styrene-*co*-butyl acrylate)-Cloisite® 30B nanocomposite containing 5.3 wt % of encapsulated Cloisite® 30B: (a) dried at room temperature, (b) heated about 80°C.[24]

TABLE I
Barrier Properties of Neat Copolymer and its Nanocomposites Containing Encapsulated Nanoclay

Nanoclay content (wt%)	Average thickness (mm)	Water uptake (%)	OTR (cm^3/m^2 24 h)	Normalized WVTR (g mm/cm^2 day)
0	0.174	3.6 (0.2)	1550	18.1 (1.0)
1.5	0.159	3.3 (0.1)	1370	16.4 (0.6)
2.56	0.172	2.9 (0.3)	1020	14.3 (0.8)
3.5	0.165	2.5 (1.5)	480	10.3 (0.4)
5.3	0.168	2.2 (0.2)	240	9.2 (0.3)

Oxygen transmission rate was measured at 23°C and 50% relative humidity.

its nanocomposites, proved that it is highly amorphous polymer. Therefore it can be concluded that the improved barrier property of the encapsulated nanocomposite films is because of the increase in the tortuous diffusion path through the prepared nanocomposite owing to the presence of exfoliated Cloisite® 30B platelets, which provides a longer path for diffusion of oxygen through the matrix. The results suggest that the barrier properties of the polymer/clay nanocmposites strongly depend on the extent of dispersed phase, as in the specimen containing 5.3% nanoclay the best barrier performance was obtained, because of the higher amount of nanoclay and therefore higher surface area. The increase in the barrier properties of the nanocomposite also reflects indirectly the dispersion state of the nanoclay in the polymeric matrix.[20] The findings prove that encapsulation of nanoclay is an effective technique to achieve exfoliation with high degree of dispersion of nanoclay within the matrix.

Water vapor transmission rate (WVTR)

Intercalation and exfoliation of clay layers produce dispersed platelets with high specific surface area, inhibiting the diffusion or flow of gases within the matrix. The data in Table I indicate that by increasing the amount of Cloisite® 30B up to 5.3 wt %, the normalized WVTR values decrease to 9.2(0.3) (g mm/cm^2 day) with respect to that of the neat copolymer 18.1(1.0) (g mm/cm^2 day). The reduction in WVTR is because of the high degree of exfoliation of encapsulated Cloisite® 30B platelets, good dispersion and high nanoclay content, which provide a tortuous path against the diffusion of water vapor molecules. Free volumes may facilitate the diffusion of the permeating molecule through the polymer. The presence of bulky styrenic side groups in the poly(styrene-*co*-butyl acrylate) results in a high free volume and therefore high permeability of the copolymer. Incorporation of the nanoclay platelets into the copolymer reduced O_2 permeability via increasing tortuosity. Although the incorporation of the nanoclay reduced both gas permeability and WVTR, there is no common relationship between gas and water permeation. Diffusion is the controlling factor in the process of gas permeation whereas in water permeation, the affinity and interaction of water molecules with the polymeric chains are influencing factors.[29] Therefore in a hydrophobic polymer, such as our copolymer, because of lack of hydrogen bonding and other chemical or physical bonding between polymer chains and water molecules a low WVTR was observed for the copolymer. Further decrease observed in WVTR of the copolymer nanocomposite is because of the tortuosity caused by incorporation of nanoclay platelets, which had already been more hydrophobic through the modification.[24]

Water uptake

Water uptake, another index of the barrier properties, was tested for the neat copolymer and its nanocomposites. According to the results (Table I), it can be concluded that nanocomposites showed lower water uptake in comparison to the neat copolymer. The reduction in the average free pathway for water molecules and lower water uptake of the modified nanoclay particles are responsible for the reduced water uptake.

Thermal properties

TGA thermograms (Fig. 3) were measured for the neat copolymer and nanocomposites at a heating rate of 10°C/min under the inert atmosphere of N_2. Thermal decomposition temperatures of all the samples were in the range of 380–450°C. The thermal stability of nanocomposites was higher than that of neat copolymer. The temperature at which 10% weight loss occurs, $T_{0.1}$, and the temperature at which 50% weight loss occurs, $T_{0.5}$, are shown in Table II. $T_{0.1}$, which is an indication of the onset of the degradation, increased from 385°C to 394°C for the nanocomposite containing 5.3 wt % encapsulated Cloisite® 30B. Similarly $T_{0.5}$, which is a measure of thermal stability, increased with the encapsulated nanoclay content from 411°C to 425°C (Table II). The

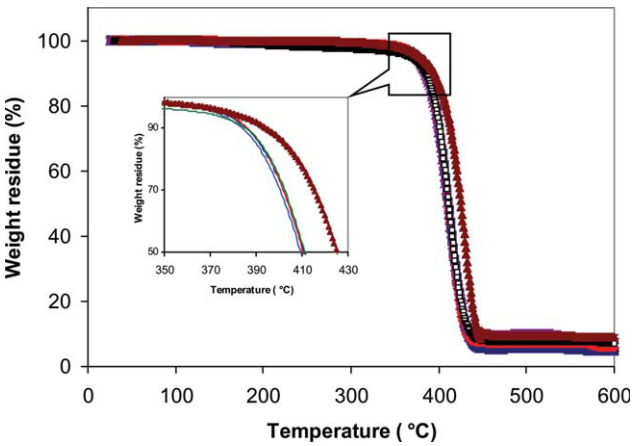

Figure 3 TGA thermograms of nanocomposites with different Cloisite® 30B contents as a function of temperature: neat copolymer (■), 1.5 wt % nanoclay (◊), 2.56 wt % nanoclay (×), 3.5 wt % nanoclay (□), 5.3 wt % nanoclay (▲). [Color figure can be viewed in the online issue, which is available at www.interscience.wiley.com.]

initial step of degradation, which has been attributed to the presence of weak linkages in the polymer chains,[30] occurs at lower temperature for neat copolymer. Evidently, the onset of thermal decomposition of these composites shifted significantly toward higher temperatures with the increase in the nanoclay content, which confirms the enhancement of thermal stability of the nanocomposite. The improved thermal stability has been attributed to the chemical interactions between polymer and nanoparticles and subsequent restricted thermal motion of polymer chains in the silicate interlayers.[31]

Incorporation of nanoclay into the polymer matrix may also act as a superior insulator and mass transport barrier to the volatile products generated during decomposition, leading to higher thermal stability.[32] The residual weight at 609°C is proportional to the organoclay content in the nanocomposite (Table II).

Mechanical properties

Typical engineering stress–strain curves for neat copolymer and nanocomposites containing 1.5, 2.56, 3.5, and 5.3 wt % encapsulated Cloisite® 30B are illustrated in Figure 4. The nanocomposites demonstrate a significant increase in Young's modulus, tensile strength, toughness, and elongation at break with increasing Cloisite® 30B content. This provides a new insight into the nanostructure of clay-reinforced nanocomposites in the encapsulated form within the polymer matrix. Although neat copolymer broke without yielding, with incorporation of 5.3 wt % encapsulated Cloisite® 30B a ductile behavior was observed in the engineering stress–strain curves. The increase in the energy at break (Table III), as an estimation of toughness, also indicates the ductile behavior of the composites. The increased elongation at break has been attributed to the strong affinity and interaction of nanofillers with polymer matrices,[33,34] which results in formation of physically cross-linked networks[35,36] or even modifications of the degree of crystallinity and crystal phase and structure.[37] The enhancement of elongation at break, Young's modulus, and tensile strength appears to be because of the strong interaction between polymeric chains and nanoclay modifier chains, which are bound to the nanoclay surfaces. The enhanced toughness could be attributed to the strong interface and the mobility of exfoliated and well dispersed nanoclay platelets within the matrix, which can blunt cracks or retard the propagation of the cracks.[37] The number of platelets that delay the crack propagation

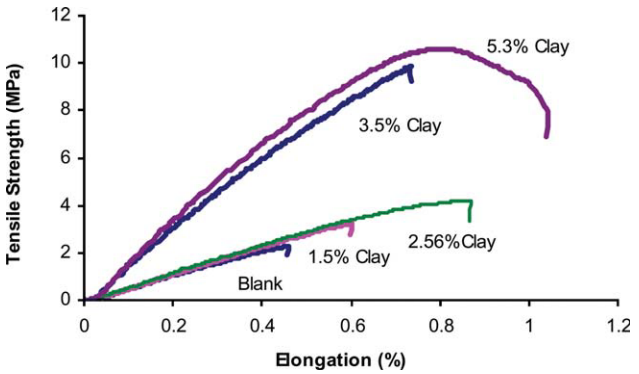

Figure 4 Typical engineering stress–strain curves for nanocomposites containing 1.5, 2.56, 3.5, and 5.3 wt % encapsulated Cloisite® 30B and blank as neat copolymer. [Color figure can be viewed in the online issue, which is available at www.interscience.wiley.com.]

TABLE II
TGA Data of Neat Copolymer and its Nanocomposites

Nanoclay content (wt %)	$T_{0.1}$ (°C)	$T_{0.5}$ (°C)	Residue at 600°C (wt %)
0	385	411	4.5
1.5	385	411	5
2.56	387	414	5.5
3.5	390	421	6.2
5.3	394	425	7.5

TABLE III
Tensile Properties and T_g of the Neat Copolymer and its Nanocomposites Containing 1.5, 2.56, 3.5, and 5.3 wt % of Encapsulated Cloisite® 30B

Nanoclay content (wt %)	Elongation at break (%)	Tensile strength (MPa)	Young's modulus (GPa)	Energy at break (J)	T_g (°C)
0	1.28	5.77	0.69	0.043	40
1.5	1.43	6.13	0.78	0.051	40
2.56	1.52	7.85	1.33	0.075	44
3.5	1.72	13.21	1.61	0.091	46
5.3	2.21	14.6	1.78	0.184	48

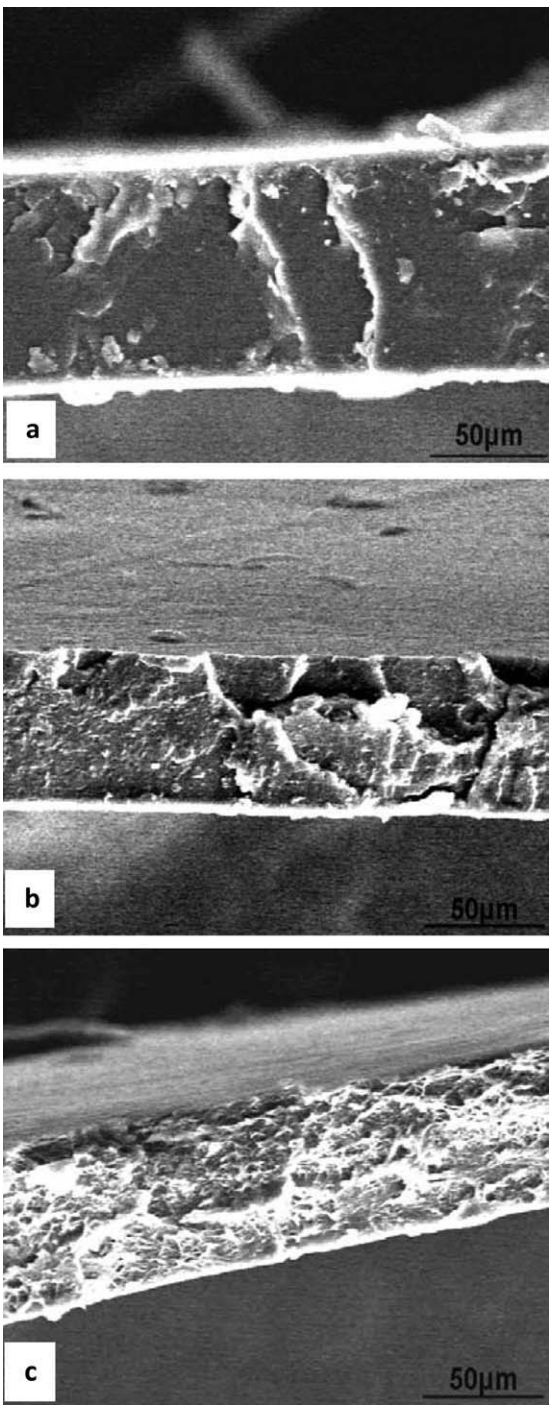

Figure 5 SEM micrographs of tensile fracture surfaces of neat copolymer (a) and nanocomposites containing: (b) 2.56 wt % and (c) 5.3 wt % nanoclay at 500× magnification.

increases by increasing the nanoclay content which results in higher toughness.[37,38] Developing new particle-filled composites to both strengthen and toughen the polymer matrices has been the interest of many researchers.[39–41] Shah and co-workers[37] observed an increase in toughness and stiffness of poly(vinylidene fluoride) nanocomposites in comparison with the neat polymer. It has been suggested that the mobility of the nanoparticles within the polymeric matrix and further nanoparticle alignment under applied tensile stress is the crucial reason of energy dissipation and the enhanced toughness of the nanocomposite. It has also been supposed that local plastic deformation of the polymer around the filler particles following debonding and crack deformation are the reasons for toughening.[42,43]

Figure 5 shows the SEM micrographs of tensile fracture surfaces of neat copolymer and nanocomposites. The remnants of local plasticity on the fracture surface of 2.56 wt % and 5.3 wt % encapsulated nanocomposites indicate that matrix has undergone more plastic deformation and ductile failure in contrast to the neat copolymer. The failure mode of matrix has been changed from almost brittle in neat copolymer to ductile with the incorporation of 5.3 wt % Cloisite® 30B. Therefore, along with the restricted mobility of polymeric chains containing encapsulated exfoliated Cloisite® 30B layers, which results in the increased modulus, the well-dispersed nanoparticles provide obstacles in the way of propagating cracks resulting in higher energy dissipation and higher toughness. The physical cross-links between the nanoclay platelets and polymer chains[36] may also be considered as a possible reason for the observed toughening and increased modulus in the nanocomposites.

Dynamic mechanical thermal analysis

Tanδ and storage modulus of neat copolymer and the nanocomposites are shown in Figure 6. An

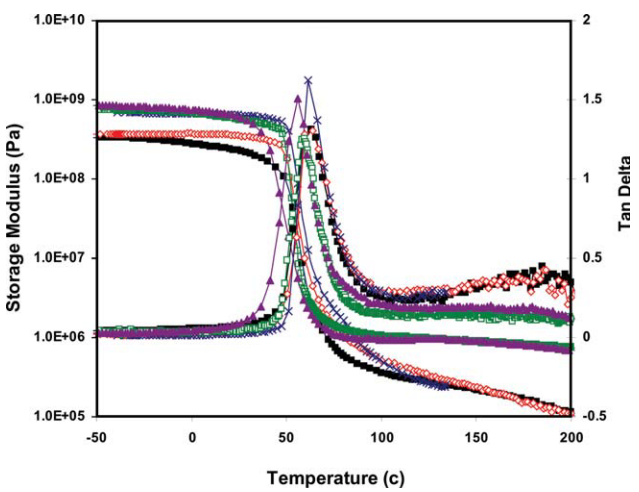

Figure 6 Tanδ and storage modulus of poly(styrene-*co*-butyl acrylate)-Cloisite® 30B nanocomposites containing different nanoclay contents with respect to temperature: neat copolymer (■), 1.5 wt % nanoclay (◊), 2.56 wt % nanoclay (×), 3.5 wt % nanoclay (□), 5.3 wt % nanoclay (▲). [Color figure can be viewed in the online issue, which is available at www.interscience.wiley.com.]

increase in the glass transition temperature was observed from about 40°C for the neat copolymer to about 48 °C for the composite containing 5.3 wt % nanoclay (Table III).

The lack of a rubber plateau region in storage modulus of the specimens containing up to 2.5 wt % indicates that the polymer is not crosslinked and/or has a molecular weight that is below or around the critical molecular weight required for physical entanglements to form. However, nanocomposites containing 3.5 and 5.3 wt % clay exhibited a rubbery plateau with G' almost independent to the temperature above the glass transition region representing the behavior of cross-linked polymers.[44] The behavior suggests that the nanoclay platelets provide physical cross-links between the copolymer chains.

CONCLUSION

The incorporation of encapsulated nanoclay platelets into poly(styrene-*co*-butyl acrylate) copolymer via miniemulsion polymerization provided nanocomposites with improved physical and mechanical properties. Interaction between matrix and nanoclay surfaces is responsible for the enhanced properties. The exfoliated nanoclay platelets provide a mode for energy dissipation as well as acting as physical cross-links, which are potential candidates for the observed enhancement of stiffness and strength. The composites provided films with significantly improved barrier properties.

References

1. Nah, C.; Ryu, H. J.; Kim, W. D.; Choi, S.-S. Polym Adv Technol 2002, 13, 649.
2. Takahashi, S.; Goldberg, H. A.; Feeney, C. A.; Karim, D. P.; Farrell, M.; O'leary, K.; Paul, D. R. Polymer 2006, 47, 3083.
3. Xu, B.; Zheng, Q.; Song, Y.; Shangguan, Y. Polymer 2006, 47, 2904.
4. Ray, S. S.; Okamoto, M. Prog Polym Sci 2003, 28, 1539.
5. Negrete-Herrera, N.; Persoz, S.; Putaux, J.-L.; David, L.; Bourgeat-Lami, E. J Nanosci Nanotech 2006, 6, 421.
6. Morsi, K.; Mcshane, H. B.; Mclean, M. Mater Sci Eng 2000, 290, 39.
7. Rajkiran, R. T.; Upendra, N. Polym Int 2008, 57, 738.
8. Sawitowski, T. Nanoadditives in paints and plastics applications, in proceedings of PIRA International Conference; Miami, FL, 2005.
9. Pinnavaia, T. J.; Beall, G. W., Eds. Polymer-clay nanocomposites, Wiley: New York, 2001.
10. Diaconu, G.; Paulis, M.; Leiza, J. R. Polymer 2008, 49, 2444.
11. Wang, Z.-Y.; Han, E.-H.; Ke, W. J Appl Polym Sci 2007, 3, 1681.
12. Hill, J.; Orr, J.; Dunne, N. Int J Nano Biomater 2008, 1, 237.
13. Krishnamoorti, R.; Vaia, R. A.; Giannelis, E. P. Chem Mater 1996, 8, 1728.
14. Mravcakova, M.; Boukerma, K.; Omastova, M.; Chehimi, M. M. Mater Sci Eng C Biomimetric Supramol Syst 2006, 26, 306.
15. Martin-Polo, M.; Mauguin, C.; Voiley, A. J Agric Food Chem 1992, 40, 407.
16. Ryan, N. M.; McNally, G. M.; Welsh, J. Dev Chem Eng Mineral Process 2004, 12, 141.
17. Dadbin, S.; Noferesti, M.; Frounchi, M. Polym Sci Tech 2008, 274, 22.
18. Salahuddin, N. Polym Composites, 2009, 30, 13.
19. Gopakumar, T. G.; Lee, J. A.; Kontopoulou, M.; Parent, J. S. Polymer 2002, 43, 5483.
20. Sun, Q.; Schork, F. J.; Deng, Y. Compos Sci Technol 2007, 67, 1823.
21. Zilg, C.; Mulhaupt, R.; Finter, J. Macromol Chem Phys 1999, 200, 661.
22. Wahit, M. U.; Hassan, A.; Mohd Ishak, Z. A.; Rahmat, A. R.; Abu Bakar, A. J Thermoplastic Compos Mater 2006, 19, 545.
23. Wu, Y.; Duan, H.; Yu, Y.; Zhang, C. J Appl Polym Sci 2001, 79, 333.
24. Mirzataheri, M.; Mahdavian, A. R.; Atai, M. Colloid Polym Sci 2009, 287, 725.
25. Piringer, O. G.; Baner, A. L., Eds. Plastic Packaging, Wiley-VCH: Weinheim, 2008.
26. Lange, J.; Wyser, Y. Packaging Technol Sci 2003, 16, 149.
27. Posey, R.; Culbertson, E. C. U.S. Pat. 6,709,735, 2004.
28. Mani, I. U.S. Pat. 4,521,494, 1985.
29. Finlayson, K. M., Ed. Plastic Film Technology, High Barrier Plastic Films for Packaging, Technomic Pub Company: Lancaster, PA, 1989; Vol. 1.
30. Kashiwagi, T.; Inaba, A.; Brown, J. E.; Hatada, K.; Kitayama, T.; Masuda, E. Macromolecules 1986, 19, 2160.
31. Blumstein, A. J Polym Sci Part A 1965, 3, 2665.
32. Zulfiqar, S.; Ahmad, Z.; Sarwar, M. L. Polym Adv Technol 2008, 19, 1720.
33. Ma, J.; Zhang, S.; Qi, Z. J Appl Polym Sci 2001, 82, 1444.
34. Chang, Y.-W.; Yang, Y.; Ryu, S.; Nah, C. Polym Int 2002, 51, 319.
35. Zhang, Z.; Zhang, L.; Li, Y.; Xu, H. Polymer 2005, 46, 129.
36. Chen, C. H.; Teng, C. C.; Yang, C. H. J Polym Sci Part:B Polym Phys 2005, 43, 1465.
37. Shah, D.; Maiti, P.; Gunn, E.; Schmidt, D. F.; Jiang, D. D.; Batt, C. A.; Giannelis, E. P. Adv Mater 2004, 16, 1173.
38. Wang, J. F.; Severtson, S. J.; Stein, A. Adv Mater 2006, 18, 1585.
39. Qu, Y. C.; Yang, F.; Yu, Z. Z. J Polym Sci Part:B Polym Phys 1998, 36, 789.
40. Lyu, S. P.; Zhu, X. G.; Qi, Z. N. J Polym Res 1995, 2, 217.
41. Margolina, A.; Wu, S. Polymer 1988, 29, 2170.
42. Argon, A. S.; Cohen, R. E. Polymer 2003, 44, 6013.
43. Gersappe, D. Phys Rev Lett 2002, 89, 058301.
44. Nielsen, L. E.; Landel, R. F. Mechanical properties of polymers and composites; 2nd ed.; Marcel Dekker, Inc.: New York, 1994.